AAS 20-705

GUIDANCE AND TRACKING CONTROL FOR RIGID BODY ATTITUDE USING TIME-VARYING ARTIFICIAL POTENTIALS

Abhijit Dongare[*], Amit K. Sanyal[†], Hossein Eslamiat[‡]
and
Sasi Prabhakaran Viswanathan[§]

This paper presents a guidance and attitude tracking control scheme in continuous time for a rigid body in SO(3), using time-varying artificial potentials. This novel idea leads to generation of an attitude trajectory that passes through desired attitude waypoints and feedback tracking of this trajectory. These waypoints can also be used for avoiding attitude or pointing direction constraints so that safe attitude navigation is ensured. Artificial time-varying potential fields at these waypoints that are attractive, are introduced. Bump functions of time, which are smooth but not real analytic, are used to generate these potentials at the desired attitude waypoints. For the terminal attitude, a different type of smooth function is used. The rigid body attitude in these time-varying potential fields gets attracted towards the desired attitude waypoints during certain time periods. This generates an attitude trajectory passing through these desired waypoints sequentially in time. A Lyapunov analysis is carried out to show stable attitude tracking through the desired waypoints and ending at the terminal attitude, using these time-varying artificial potentials. Numerical simulations are carried out to test the performance of this attitude guidance and tracking scheme.

INTRODUCTION

Guidance and control of rigid body is an essential problem for aerospace, underwater and ground vehicles. This work proposes a novel scheme for attitude trajectory generation and tracking control. The method involves guidance and trajectory tracking of rigid body attitude from a given initial attitude to a given final (rest) attitude through a set of intermediate attitude waypoints. This scheme is based on the use of time-varying artificial potential fields.

Trajectory generation is an essential problem for operations of an autonomous vehicle. It requires complete information regarding the geometry of the rigid body, its surroundings, and its dynamics. Path planning for collision avoidance is described in.[1] Artificial potentials have been used as a way for collision avoidance.[2] Collision avoidance can be distributed among several levels of control as described in[3] and[4] instead of just as a high level problem. This significantly helps to increase the safety in real-time operations. Obstacles detected can be avoided by constructing repulsive artificial potential fields around them, and destinations and waypoints are represented as attractive potentials. The concept of artificial potentials has also been used in robot path planning.[5] The artificial potential function can be designed to include information on the environment and the aim.

[*]Ph.D. Student, Department of Mechanical and Aerospace Engineering, audongar@syr.edu.
[†]Associate Professor, Department of Mechanical and Aerospace Engineering, aksanyal@syr.edu.
[‡]Ph.D. Student, Department of Mechanical and Aerospace Engineering, heslamia@syr.edu.
[§]Akrobotix LLC, Syracuse, New York.

Guidance for multiple robots can also be carried out using artificial potentials.[6] Artificial potentials can be used for fast and efficient path planning by prioritizing robots accordingly.

Artificial potentials have also been applied in spacecraft formation control.[7] A scheme for autonomous rendezvous in orbit with a target can be designed using an artificial potential function.[8] Spacecraft collision avoidance during a rendezvous maneuver using an artificial potential for guidance and sliding mode control for tracking is another application.[9] Artificial potential using relative orbital elements to achieve a relative orbit was treated in.[10] Another application of artificial potential is for in orbit servicing.[11] This concept uses a simple attractive and a dynamic repulsive artificial potential, which prioritizes obstacles to avoid by assigning weight factors. Applications to formation control for multiple unmanned aerial vehicles are discussed in[12] and.[13] The former paper describes formation tracking control in a constrained space. It uses the formation potential field which is a modified artificial potential field that maintains the formation along with collision avoidance among the vehicles and also the surroundings. The latter paper describes a formation potential field for formation control and collision avoidance in dynamic environments. Another approach involves use of logarithmic barrier potentials in terms of quaternions, for spacecraft attitude control in order to avoid constraints and remain in certain zones.[14]

This work uses the framework of geometric mechanics along with time-varying artificial potential fields to guide a rigid body through desired attitude waypoints and settle into a desired final rest attitude. The concepts of "virtual leaders" along with artificial potentials on the Lie group of rigid body motions in three dimensional Euclidean space is used to control multiple autonomous vehicles.[15] Spacecraft formation control in the framework of geometric mechanics can be done using artificial potentials and a virtual leader.[16] Artificial potentials is also used for collision avoidance in Riemannian manifolds.[17] The work in[18] involves geometric control of attitude using both attractive and repulsive potentials for guidance. The desired attitude is obtained asymptotically while avoiding undesirable orientations. The novelty of this work is that it uses time-varying artificial potentials for guidance through desired waypoints on the Lie group $\mathrm{SO}(3)$ of rigid body attitude. Further, the time-varying artificial potentials used here are defined only on closed (compact) intervals of time, designed to coincide with time intervals at which the desired waypoints should be reached.

The outline of this manuscript has four main sections. The first Section describes attitude dynamics of a rigid body on $\mathrm{SO}(3)$. The second Section describes the design of attractive time-varying artificial potential fields for reaching attitude waypoints, and repulsive potentials to avoid undesirable zones. It also gives a (continuous time) control law for attitude tracking, along with a Lyapunov analysis to show its stability. The fourth Section involves numerical simulation results using a Lie group variational integrator scheme that was used in.[19] The final section provides concluding remarks and explores possible future research directions.

PROBLEM FORMULATION

Coordinate Frame Definition

The configuration space of rigid body attitude motion is the Lie group $\mathrm{SO}(3)$. The attitude is described by a rotation matrix relating a body-fixed coordinate frame to an inertial coordinate frame. We consider a coordinate frame $\mathcal{B}$ fixed to the body and another coordinate frame $\mathcal{I}$ that is fixed in space and takes the role of an inertial coordinate frame. Let $R \in \mathrm{SO}(3)$ denote the orientation (attitude) of the body, defined as the rotation matrix from frame $\mathcal{B}$ to frame $\mathcal{I}$.

Rigid Body Attitude Dynamics with Control Input Torque

The model for attitude dynamics of a rigid body acting under a control torque is outlined here. The attitude of the rigid body is given by the rotation matrix $R \in \mathrm{SO}(3)$ from body-frame coordinate frame to an inertial frame. The angular velocity of the rigid body is represented in body-fixed frame and is denoted by $\Omega \in \mathbb{R}^3$. The attitude kinematics is given by

$$\dot{R} = R\Omega^{\times}, \tag{1}$$

where $(\cdot)\colon \mathbb{R}^3 \to \mathfrak{so}(3)$ is the skew-symmetric cross product operator and $\mathfrak{so}(3)$ is the Lie algebra of $\mathrm{SO}(3)$, identified with the linear space of 3×3 skew-symmetric matrices. Note that the cross-product operator is given by:

$$x^{\times} = \begin{bmatrix} x_1 \\ x_2 \\ x_3 \end{bmatrix}^{\times} = \begin{bmatrix} 0 & -x_3 & x_2 \\ x_3 & 0 & -x_1 \\ -x_2 & x_1 & 0 \end{bmatrix}. \tag{2}$$

The attitude dynamics is given by

$$J\dot{\Omega} = -\Omega \times J\Omega + \tau_c, \tag{3}$$

where J is the inertia matrix of the body expressed in the body-fixed coordinate frame and $\tau_c \in \mathbb{R}$ is the control input torque which is applied to the rigid body about its center of mass. The rigid body here is considered to be stationary in terms of translational motion.

Attitude Waypoint Navigation

The goal of the attitude waypoint navigation is to enable smooth reorientation of the rigid body from its initial attitude to the desired final attitude. This navigation is realized by a given finite set of attitude waypoints through which the rigid body is required to reorient itself. These waypoints are given in the form of rotation matrices from body-fixed frame $\mathcal{B}$ to inertial frame $\mathcal{I}$ ordered according to a strictly increasing sequence of time instants, as follows:

$$\begin{aligned} &R_{d_1}, R_{d_2}, ..., R_{d_n} \in \mathrm{SO}(3), \\ &\text{with } R_{d_i} = R_d(t_i) \in \mathrm{SO}(3) \text{ and } t_1 < t_2 < ... < t_n. \end{aligned} \tag{4}$$

Here, $R_{d_1}, R_{d_2}, ..., R_{d_{n-1}}$ are the intermediate attitude waypoints and $R_{d_n} = R_f$ is the final attitude waypoint.

TIME-VARYING ARTIFICIAL POTENTIAL

The approach for guidance and navigation of the rigid body attitude, with equations (1) and (3) describing its attitude motion, is formulated here. A bump function is used to design a time-varying artificial potential function for attitude guidance, as described here. The artificial potential function is designed as the product of a time-varying bump function that has compact support in time, and a Morse function on the Lie group of rigid body rotations. A Morse function is a non-degenerate function with a disjoint set of critical points.[20] Positive definite Morse functions form the best candidates for Lyapunov functions on *non-contractible* manifolds, i.e., spaces that cannot

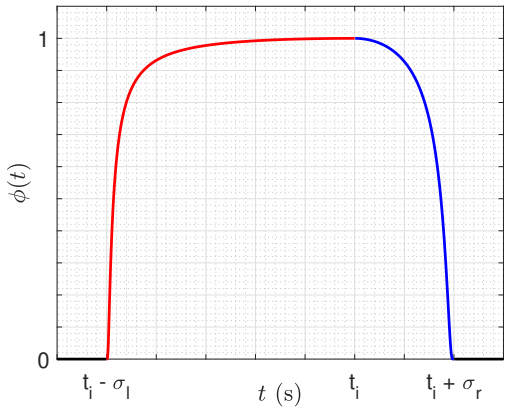

Figure 1: Asymmetric Bump Function

be contracted continuously to a point. The stability analysis of the overall guidance and tracking control is carried out to show stable trajectory generation through these waypoints, using Lyapunov analysis with a time-varying Morse-Lyapunov function.

Bump Functions for Intermediate Waypoints

At each intermediate attitude waypoint, we design a time-varying function to describe the potential field. This is in the form of a smooth bump function that is positive in a compact time interval and zero outside this interval. This function starts from zero and smoothly reaches a finite maximum (positive) value in a finite time period, before smoothly decaying to zero in finite time. The finite time periods of rise and decay are the one-sided widths of this function. These widths on either side of the function can be equal or different. We call the left side of the bump function as a "smooth step-up" function and the right side of the bump function as a "smooth step-down" function. The function depicted in Fig. 1 has different widths on either side, and hence this bump function is asymmetrical.

Consider an i^{th} asymmetrical bump function $\phi_i \colon \mathbb{R} \to \mathbb{R}$ that is smooth[21,22] and compactly supported, given by

$$\phi_i(t) = \begin{cases} e^{\dfrac{-k_{l_i}\Delta t_i^2}{\sigma_{l_i}^2(\sigma_{l_i}^2 - \Delta t_i^2)}} & t \in (t_i - \sigma_{l_i}, t_i] \\ e^{\dfrac{-k_{r_i}\Delta t_i^2}{\sigma_{r_i}^2(\sigma_{r_i}^2 - \Delta t_i^2)}} & t \in (t_i, t_i + \sigma_{r_i}) \\ 0 & \text{elsewhere,} \end{cases} \tag{5}$$

where $\Delta t_i = t - t_i$, σ_{l_i} is the width of the left side of the bump function and σ_{r_i} is the width of the right side of the bump function. The k_{l_i} and k_{r_i} are the scalar control gains that control the steepness of the left and right side of the bump function respectively. The time instant t_i is the time when the rigid body reaches corresponding desired attitude waypoint R_{d_i}. The maximum value of this bump function is unity when $t = t_i$. The derivative of the left side of the asymmetric bump

function is given by:

$$\dot{\phi_{l_i}}(t) = -2k_{l_i}\Delta t_i \left(\frac{1}{\sigma_{l_i}^2(\sigma_{l_i}^2 - \Delta t_i^2)} + \frac{\Delta t_i^2}{\sigma_{l_i}^2(\sigma_{l_i}^2 - \Delta t_i^2)^2} \right) e^{\frac{-k_{l_i}\Delta t_i^2}{\sigma_{l_i}^2(\sigma_{l_i}^2 - \Delta t_i^2)}}. \tag{6}$$

Note that $\dot{\phi_{l_i}}(t)$ is positive as $t - t_i$ is negative. Similarly the derivative of the right side of the bump function is given by:

$$\dot{\phi_{r_i}}(t) = -2k_{r_i}\Delta t_i \left(\frac{1}{\sigma_{r_i}^2(\sigma_{r_i}^2 - \Delta t_i^2)} + \frac{\Delta t_i^2}{\sigma_{r_i}^2(\sigma_{r_i}^2 - \Delta t_i^2)^2} \right) e^{\frac{-k_{r_i}\Delta t_i^2}{\sigma_{r_i}^2(\sigma_{r_i}^2 - \Delta t_i^2)}}, \tag{7}$$

and the derivative is negative since $t - t_i$ is positive in this case.

Smooth Step-Down Function for Initial Attitude

We use a "smooth step-down" function for the initial attitude at time $t = 0$, which starts at a constant value of 1 (for $t \leq 0$) and thereafter decays to 0 in finite time, as follows:

$$\phi_b(t) = \begin{cases} 1 & t \in (-\infty, 0) \\ e^{\frac{-k_b t^2}{\sigma_b^2(\sigma_b^2 - t^2)}} & t \in [0, \sigma_b), \end{cases} \tag{8}$$

where $t \in [0, \sigma_b)$ and σ_b is the width of this function. The derivative of this function (for $t \geq 0$) is,

$$\dot{\phi_b}(t) = -2k_b t \left(\frac{1}{\sigma_b^2(\sigma_b^2 - t^2)} + \frac{t^2}{\sigma_b^2(\sigma_b^2 - t^2)^2} \right) e^{\frac{-k_b t^2}{\sigma_b^2(\sigma_b^2 - t^2)}}. \tag{9}$$

Smooth Step-Up Function for Final Waypoint

The bump functions used to go through the intermediate attitude waypoints are "two-sided", i.e., they rise from 0 smoothly to a maximum value of 1 and then decay smoothly back to 0. But for the final waypoint we need only a "smooth step-up" function that starts with zero and rises to the maximum value of 1 and settles there. Consider the following function:

$$\phi_f(t) = \begin{cases} e^{\frac{-k_f \Delta t_f^2}{\sigma_f^2(\sigma_f^2 - \Delta t_f^2)}} & t \in (t_f - \sigma_f, t_f] \\ 1 & t \in (t_f, \infty), \end{cases} \tag{10}$$

where σ_f is the width of this function, k_f is the parameter to control the steepness of the function, t_f is the time when the rigid body reaches its final waypoint. The time derivative of this function, which is positive in the time interval $(t_f - \sigma_f, t_f)$, is given by:

$$\dot{\phi_f}(t) = -2k_f \Delta t_f \left(\frac{1}{\sigma_f^2(\sigma_f^2 - \Delta t_f^2)} + \frac{\Delta t_f^2}{\sigma_f^2(\sigma_f^2 - \Delta t_f^2)^2} \right) e^{\frac{-k_f \Delta t_f^2}{\sigma_f^2(\sigma_f^2 - \Delta t_f^2)}}. \tag{11}$$

Attractive Potential

We define the attitude tracking error for the i^{th} desired attitude waypoint as $Q_i = R_{d_i}^{\mathrm{T}} R(t)$ for $t \in [t_{i-1}, t_i]$. As the rigid body approaches the i^{th} desired attitude waypoint, the corresponding attitude error Q_i decays to zero. Once the attitude waypoint is achieved, the rigid body then again reorients itself to achieve the next waypoint. Thus, the rigid body passes through the series of reorientations. The attitude error thus goes to zero in piecewise manner. This continues to occur, till the rigid body achieves it's final attitude and then stabilizes. The attractive potential $AP(Q,t)\colon \mathrm{SO}(3)\times\mathbb{R}^+ \to \mathbb{R}^+$ is given by the following Morse function,[23]

$$AP_i(Q_i, t) = \langle K_i(t), I - Q_i \rangle, \tag{12}$$

where $K_i(t) = \phi_i(t) K_o$ and $K_o = \mathrm{diag}(K_1, K_2, K_3)$ and $\phi_i(t)$ is a bump function. The positive diagonal matrix K_o consists of control gain values $K_1, K_2, K_3 > 0$ and are unique. Representation of the attractive potential is given in Fig. 2. This value reaches its minimum value of zero as $Q_i \to I$.

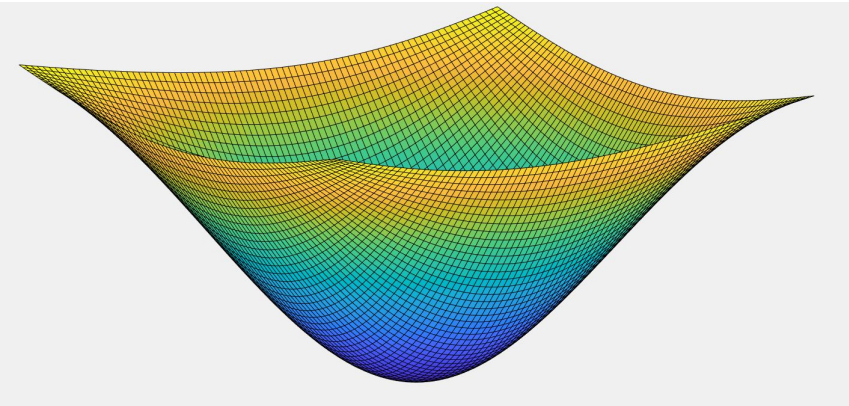

Figure 2: Attractive Potential

Repulsive Potential

The attractive potential is used to attract the rigid body to a desired attitude. Similarly, a repulsive potential[18] is used to avoid undesirable orientations. The rigid body should be able to avoid these undesirable attitudes at all times. This paper assumes that the undesirable attitudes are present at all times and are not changing. Hence, the function is not explicitly time-varying. This potential function has non-negative values ranging from zero to infinity as the rigid body approaches the undesirable orientation. The repulsive potential is an analytic function that is given by the following exponential function,

$$RP(R(t)) = e^{\frac{f}{\cos(\Psi) - r^T R^T \upsilon}} - 1, \tag{13}$$

where $r \in \mathbb{S}^2$ is the unit vector (in body frame) specifying the pointing direction of the sensor, and $\upsilon \in \mathbb{S}^2$ is the vector (in inertial frame) pointing towards an undesirable direction. The term $r^T R^T \upsilon$ specifies the angle between the sensor pointing direction and the direction vector to be avoided. The angle Ψ is the required minimum angular separation between them such that $\Psi \in (0, \pi/2)$. The positive constant f controls the shape of the function. The compact support of the repulsive

potential (on $\mathrm{SO}(3)$) decreases as the value of f decreases. This ensures that the effect due to the repulsive potential vanishes beyond the neighborhood of the minimum angular separation for the undesirable direction. We enforce the condition of zero exposure of the sensor to the undesirable zone. The above condition can be exercised with following constraint,

$$\cos(\Psi) - r^T R^T \upsilon > 0. \tag{14}$$

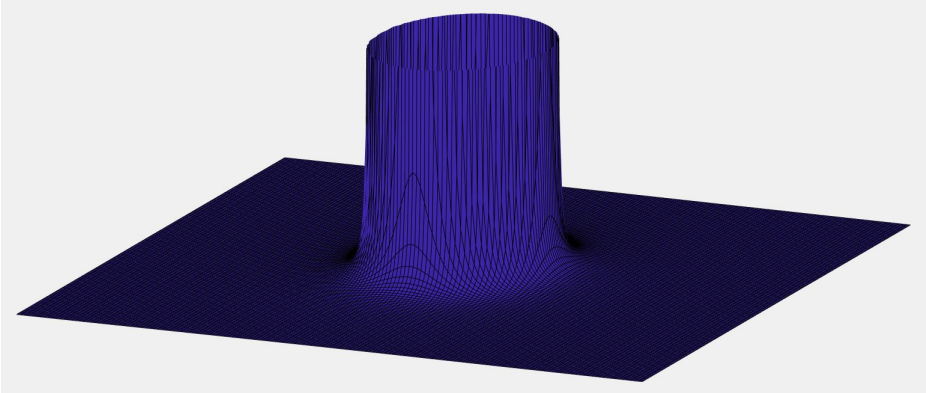

Figure 3: Repulsive Potential

The repulsive potential is illustrated in Fig. 3 .

The Potential Function

The potential function is the sum of attractive and repulsive potential functions. Let $R_{d_i} \in \mathrm{SO}(3)$ denote an intermediate desired attitude at time t_i. The potential function is given by:

$$U(Q_i, t) = \sum_{i=1}^{n} AP_i(Q_i, t) + RP(R(t)), \tag{15}$$

where $AP_i(Q_i, t)$ and $RP(R(t))$ are given by equations (12) and (13), respectively. The potential function is explicitly time-dependent. The attractive potential is $AP_i(Q_i, t) = 0$, when $Q_i = I$. Additionally, the bump function for a particular desired attitude waypoint is positive only in the respective time intervals. Outside those time intervals the attractive potential is not acting and equal to zero. Unlike the attractive potential, the repulsive potential is not time-varying and it is always acting. From the condition in equation (14), we see that the repulsive potential is always positive. Hence we can conclude that the potential function is a positive definite function at all times. The derivative of the above potential function is given by:

$$\frac{d}{dt}U(Q_i, t) = \sum_{i} \frac{d}{dt}AP_i(Q_i, t) + \frac{d}{dt}RP(R(t)), \tag{16}$$

$$\frac{d}{dt}U(Q_i, t) = \sum_{i} (\langle \dot{K}_i(t), I - Q_i \rangle + S_{K(t)}(Q_i^{\mathrm{T}})\Omega) + \rho \cdot \Omega. \tag{17}$$

where ρ is given by

$$\rho = \left(\frac{-f(R^{\mathrm{T}}v)^{\times} r}{(\cos(\Psi) - r^{\mathrm{T}} R^{\mathrm{T}} v)^2} e^{\frac{f}{\cos(\Psi) - r^{\mathrm{T}} R^{\mathrm{T}} v}} \right), \tag{18}$$

$S_{K(t)}(Q_i) = \mathrm{vex}(K_i(t)Q_i - Q_i{}^{\mathrm{T}} K_i(t))$ and $\mathrm{vex}(\cdot)\colon \mathfrak{so}(3) \to \mathbb{R}^3$ is the inverse of the $(\cdot)^{\times}$ map.

Design of the Control Law

Theorem 1. *Consider the attitude kinematics and dynamics of a rigid body given by eqs. (1)-(3). Let t_i and R_{d_i} denote the sequences of time instants and desired attitude waypoints at these instants, as defined by (4), and let $Q_i(t) = R_{d_i}^{\mathrm{T}} R(t)$ for $t \in (t_{i-1}, t_i]$ be the attitude error, as defined earlier. Define*

$$L_0(t) = \begin{cases} \dot{\phi}_{i_l}(t) & \in (t_i - \sigma_{i_l}, t_i] \\ \dot{\phi}_f(t) & \in (t_f - \sigma_f, t_f] \\ 0 & \textit{elsewhere}, \end{cases} \tag{19}$$

where $\dot{\phi}_{i_l}$ and $\dot{\phi}_f$ are the derivatives of the smooth functions defined in equations (6) and (11) respectively. The time instants t_i and t_f are those at which the rigid body reaches the intermediate attitude waypoints and the final waypoint. Let $L(t)$ be the positive definite matrix such that $L(t) = L_0(t)I + J$, where $L_0(t)$ is positive semidefinite. Define the control law as

$$\tau_c = -S_{K(t)}(Q_i) - \rho - L(t)\Omega, \tag{20}$$

where ρ is as defined in (18), $S_{K_i(t)}(Q_i) = vex(K_i(t)Q_i - Q_i^{\mathrm{T}} K_i(t))$, and $vex(\cdot)\colon \mathfrak{so}(3) \to \mathbb{R}^3$ is the inverse of the $(\cdot)^{\times}$ map. The control law (20) then stabilizes the attitude dynamics of the rigid body to $(R, \Omega) = (R_f, 0)$.

Proof. Consider the following (candidate) Morse-Lyapunov function:

$$V(Q_i, \Omega, t) = \frac{1}{2}\Omega^{\mathrm{T}} J\Omega + U(Q_i, t), \tag{21}$$

defined piecewise on the time interval $(t_{i-1}, t_i]$. It can be seen that $V(Q_i, \Omega, t)$ is a positive definite function. Using equation (16) the derivative of the above Morse-Lyapunov function is given by:

$$\dot{V} = \Omega^{\mathrm{T}} J\dot{\Omega} + \frac{d}{dt} U(Q_i, t). \tag{22}$$

Using equation (3) we have the following:

$$\dot{V} = \Omega^{\mathrm{T}} \left(J\Omega \times \Omega + \tau_c + S_{K(t)} Q_i \right) + \rho \cdot \Omega + \dot{\phi}_i(t) \langle K_o, I - Q_i \rangle. \tag{23}$$

Substituting the control law from equation (20), we get,

$$\begin{aligned} \dot{V} &= -\Omega^{\mathrm{T}} L(t)\Omega + \dot{\phi}_i(t) \langle K_o, I - Q_i \rangle \\ &= -\Omega^{\mathrm{T}} (L_0(t)I + J)\Omega + \dot{\phi}_i(t) \langle K_o, I - Q_i \rangle. \end{aligned} \tag{24}$$

As the second term on the right hand side in the derivative of the Lyapunov function in eq. (24) is non-definite, it may need to be compensated by the negative first term. However, as this term is transient in nature, we design the $L_0(t)$ to mimic the increasing and decreasing portions of $\dot{\phi}_i(t)$ in order to compensate its effect over the time interval $(t_{i-1}, t_i]$.

When the rigid body approaches the final desired attitude, the attractive potential will have $\phi_f(t)$ as the "smooth step-up" function. As the derivative $\dot{\phi}_f(t)$ is positive, the term $\dot{\phi}_f(t)\langle K_o, I - Q_f\rangle$ will be positive in the time interval $(t_f - \sigma_f, t_f]$. So we design $L_0(t) = \dot{\phi}_f(t)$ to compensate for this effect during this transient time interval when $\dot{\phi}_f(t)$ is not zero. This ensures that the transient effects are mitigated and the attitude error $Q_f = I$ when $t = t_f$. For time is $t > t_f$, $\dot{\phi}_f(t)$ is zero. As a result, we get

$$\dot{V} = -\Omega^{\mathrm{T}} J\Omega \;\forall\, t > t_f. \tag{25}$$

Therefore, using the invariance principle on the state space $\mathrm{TSO}(3)$, we can conclude that (R, Ω) converges locally asymptotically to $(R_f, 0)$.

The attractive potential function has a global minimum value when $R = R_f$ and $t = t_f$. Thus, the global minimum is with respect to $R \in \mathrm{SO}(3)$ and $t \in \mathbb{R}_+$. The repulsive potential has a global maximum with respect to $R \in \mathrm{SO}(3)$ in the undesirable zone, i.e. in the region where $\Psi > \cos^{-1}(r^{\mathrm{T}} R^{\mathrm{T}} \upsilon)$ From the equation of repulsive potential (13), we can conclude that when $r^{\mathrm{T}} R^{\mathrm{T}} \upsilon \to \cos(\Psi)$, then the potential function $U \to \infty$. As, the rigid body approaches towards the undesirable zone, the control torque generates large repulsive torques. Thus, the rigid body reorients itself away from the undesirable zone and towards the global minimum.

□

NUMERICAL SIMULATION RESULTS

This section gives some simulation results to demonstrate the potential function formulated in the earlier section. For the purpose of simulation one intermediate waypoint is considered.

Discretized Equations of Motion

For this simulation, the continuous dynamics and kinematics equations are replaced by the corresponding discretized equations of motion. A Lie group variational integrator (LGVI) is used for discretizing the continuous equations of motion. A LGVI preserves the structure of the configuration space, which in this case is the Lie group $\mathrm{SO}(3)$, without any parametrization or reprojection. Variational Integrators[24] are a class of numerical integrators which conserve the momentum map and symplectic structure when the dynamics is almost conservative or fully conservative. The discrete equations of motion for Lie Group Variational Integrator scheme are given by,[25]

$$\begin{aligned} R_{k+1} &= R_k F_k, \\ J\Omega_{k+1} &= F_k^T J\Omega_k + h\tau_k, \end{aligned} \tag{26}$$

where h is the fixed time step such that $h = t_{k+1} - t_k$, subscript k is the k^{th} time step of the simulation and $F_k \approx \exp(h\Omega_k^{\times}) \in \mathrm{SO}(3)$ guarantees that R_k evolves on $\mathrm{SO}(3)$.

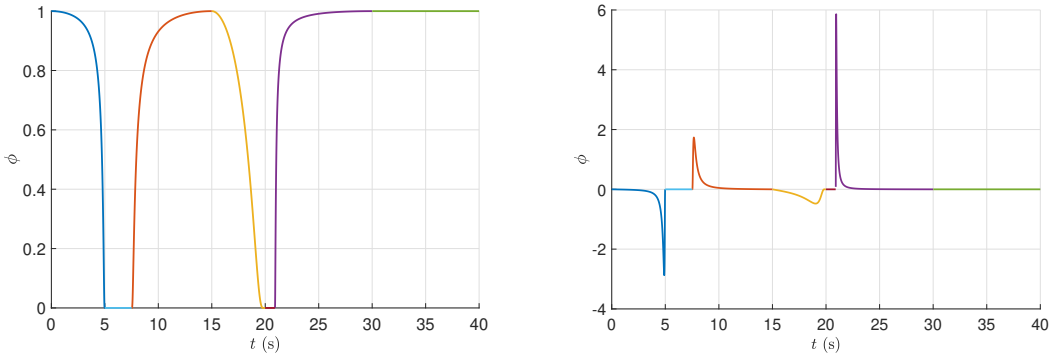

Figure 4: Bump function (left) and it's derivative (right).

Numerical Simulation

The time-varying artificial potential scheme presented in this paper is simulated for a rigid body navigating around one undesirable zone towards its final orientation. This simulation has one intermediate and one final desired attitude waypoint. The simulation for the above scheme assumes the inertia matrix as $J = \text{diag}(0.08, 0.15, 0.19)$ kgm^2. The direction of sensor in body-fixed frame is given by $r = [1, 0, 0]^{\mathrm{T}}$. The initial attitude is given by $R^o = \exp([0, 0, 150\text{x}(\pi/180)]^{\mathrm{T}})$ and the desired final attitude is $R^F = \exp([0, 0, 0]^{\mathrm{T}})$. Finally, $R^I = \exp([0, 0, 90\text{x}(\pi/180)]^{\mathrm{T}})\text{x}\exp([0, 7\text{x}(\pi/180), 0]^{\mathrm{T}})$ defines the one intermediate waypoint. The undesirable zone is located at $\exp([0, 0, 45\text{x}(\pi/180)]^{\mathrm{T}})\text{x}$ $\exp([0, 10\text{x}(\pi/180), 0]^{\mathrm{T}})$. The minimum angular separation is $\Psi = 15^o$. The time step is $h = 0.01$s and the diagonal gain matrix is $K_o = \text{diag}(0.05, 0.0095, 0.159)$.

The simulation begins at $t_0 = 0$s and ends at $t_E = 40$s. The rigid body reaches the intermediate waypoint at $t_1 = 15$s and the final waypoint at $t_f = 30$s. Once the rigid body achieves the desired final waypoint at $t_f = 30$s, the rigid body then maintains its final attitude. The bump function for this simulation and its corresponding derivative is shown in Fig. 4 The results of the numerical simulation are summarized in Fig. 5

In Fig. 5a, at $t = 0$s the attitude tracking error plot shows the error between current attitude and first desired attitude waypoint. This error is almost zero when time approaches 15 s as the rigid body moves closer to the desired intermediate attitude waypoint. After $t = 15$s the attitude error increases instantaneously to a finite value as the new desired attitude, which is the final desired attitude, becomes the new goal. Thus, the attitude error goes to zero in a piecewise manner as expected. At $t = 30$s, the rigid body achieves its final attitude and stabilizes there. The Fig. 6 shows the shows the pointing direction of the sensor in the inertial frame, which is represented as an unit vector on $\mathbb{S}^2$.

CONCLUSION

In this paper an integrated attitude guidance and tracking scheme that utilizes time-varying artificial potential functions, is proposed. This continuous time scheme is designed directly on the configuration space of rigid-body attitude motion, $\text{SO}(3)$. The scheme can generate a desired attitude trajectory through multiple attitude waypoints and then track that desired trajectory through the waypoints. The guidance of the rigid body is achieved by assigning attractive time-varying artificial potentials to desired attitude waypoints, while avoiding undesirable orientations using repulsive

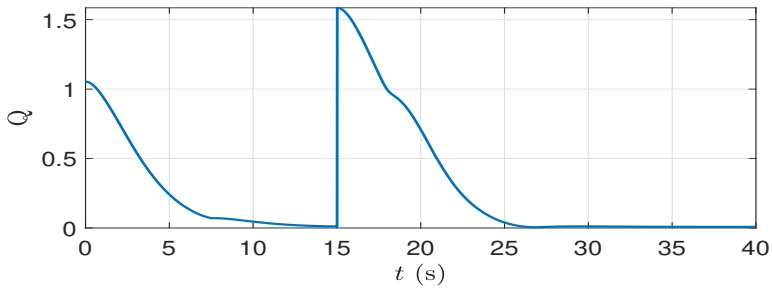

(a) Attitude Error

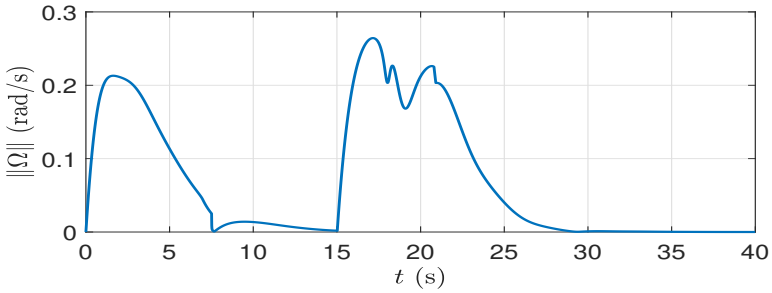

(b) Angular Velocities

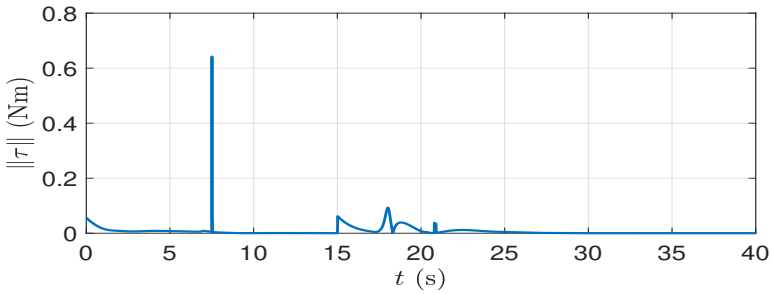

(c) Control torque

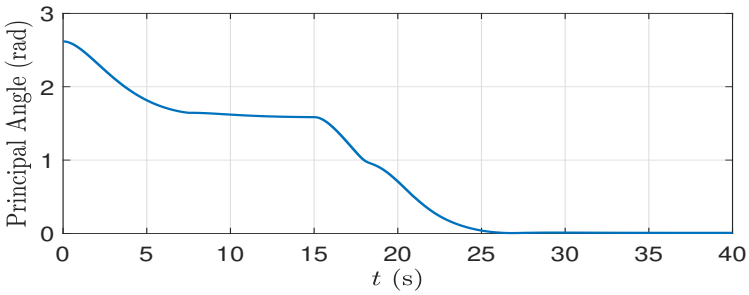

(d) Principal Angle

Figure 5: Simulation Results

potentials. These attractive potentials are generated using asymmetric bump functions of time. A possible future research direction is to consider the full translational and rotational motion of rigid-bodies in $\mathrm{SE}(3)$ and create an integrated guidance and control scheme for this full motion. Another

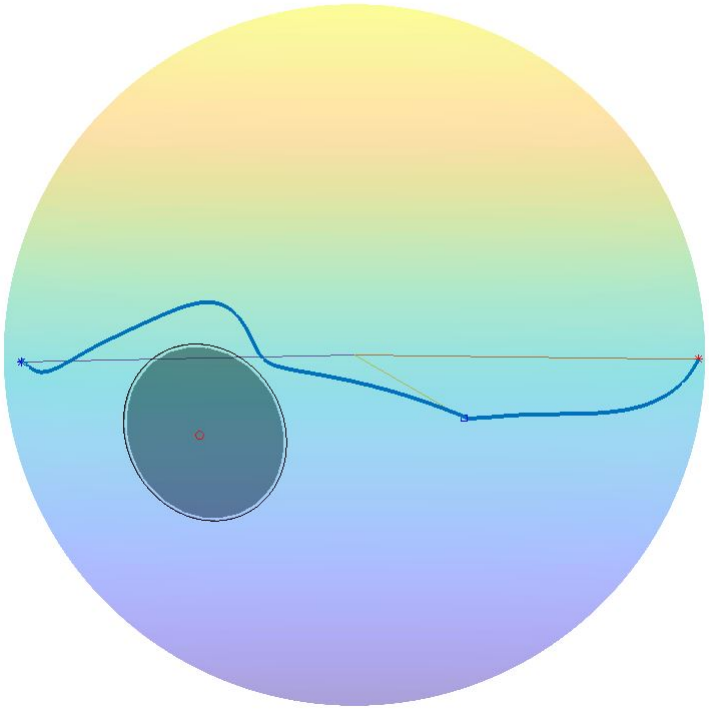

Figure 6: Trajectory of sensor fixed in body-frame

research direction is to extend the above scheme to undesirable zones which are dynamic in nature.

ACKNOWLEDGEMENT

The authors acknowledge support from the National Science Foundation awards CISE 1739748 and IIP 1938518 (SBIR through Akrobotix, LLC).

REFERENCES

[1] T. Lozano-Perez, "Spatial Planning: A Configuration Space Approach," *IEEE Transactions on Computers*, Vol. C-32, IEEE, 1983, pp. 108–120.

[2] O. Khatib and J. F. L. Maitre, "Dynamic control of manipulators operating in a complex environment," *On Theory and Practice of Robots and Manipulators, 3rd CISM-IFToMM Symp*, Vol. 267, 1978.

[3] O. Khatib, "Real-time obstacle avoidance for manipulators and mobile robots," *Proceedings. 1985 IEEE International Conference on Robotics and Automation*, 1985.

[4] O. Khatib, *The Potential Field Approach And Operational Space Formulation In Robot Control*. Springer, 1986.

[5] E. Rimon and D. E. Koditschek, "Exact Robot Navigation Using Artificial Potential Functions," *IEEE Transactions on Robotics and Automation*, Vol. 8, IEEE, 1992.

[6] C. W. Warren, "Multiple robot path coordination using artificial potential fields," *Proceedings. IEEE International Conference on Robotics and Automation*, IEEE, 1990.

[7] S. Renevey and D. A. Spencer, "Spacecraft Formations Using Artificial Potential Functions and Relative Orbital Elements," *29th AAS/AIAA Space Flight Mechanics Meeting,*, 2019.

[8] I. Lopez and C. R. McInnes, "Autonomous Rendezvous Using Artificial Potential Function Guidance," *Journal of Guidance, Control, and Dynamics*, Vol. 18, No. 2, 1995, pp. 237–241.

[9] E. C. M. Mancini, N. Bloise and E. Punta, "Sliding Mode Control Techniques and Artificial Potential Field for Dynamic Collision Avoidance in Rendezvous Maneuvers," *IEEE Control Systems Letters*, Vol. 4, No. 2, 2020, pp. 313–318.

[10] D. A. Spencer, "Automated Trajectory Control Using Artificial Potential Functions to Target Relative Orbits," *Journal of Guidance, Control, and Dynamics*, Vol. 39, No. 9, 2016, pp. 1–7.

[11] A. Tatsch and N. Fitz-Coy, "Dynamic Artificial Potential Function Guidance for Autonomous On-Orbit Servicing," *6th International ESA Conference on Guidance, Navigation and Control Systems*, Vol. 606, 2006.

[12] H. Yin, L. L. Cam, and U. Roy, "Formation control for multiple unmanned aerial vehicles in constrained space using modified artificial potential field," *Math. Model. Eng. Probl*, Vol. 4, No. 2, 2017, pp. 100–105.

[13] I. Skyrda, V. Chepizhenko, and T. Davydenko, "Formation Control of Multiple Autonomous Fixed-Wing Unmanned Aerial Vehicles in Dynamic Environment," *Archived Volume*, 2019, p. 178.

[14] U. Lee and M. Mesbahi, "Spacecraft Reorientation in Presence of Attitude Constraints via Logarithmic Barrier Potentials," *in American Control Conference*, 2011, pp. 450–455.

[15] N. E. Leonard and E. Fiorelli, "Virtual leaders, artificial potentials and coordinated control of groups," Orlando, FL, Dec. 2001, pp. 2968–2973.

[16] D. Lee, A. K. Sanyal, and E. A. Butcher, "Asymptotic Tracking Control for Spacecraft Formation Flying with Decentralized Collision Avoidance," *Journal of Guidance, Control, and Dynamics*, Vol. 38, No. 4, 2015, pp. 587–600, 10.2514/1.G000101.

[17] M. Assif, R. Banavar, A. Bloch, M. Camarinha, and L. Colombo, "Variational collision avoidance problems on Riemannian manifolds," *2018 IEEE Conference on Decision and Control (CDC)*, IEEE, 2018.

[18] S. Kulumani and T. Lee, "Constrained Geometric Attitude Control on SO(3)," *International Journal of Control, Automation and Systems*, Vol. 15, No. 6, 2017.

[19] M. L. T. Lee and N. H. McClamroch, "A Lie group variational integrator for the attitude dynamics of a rigid body with applications to the 3D pendulum," *IEEE Conference on Control Applications*, IEEE, 2005, pp. 962—-967.

[20] J. Milnor, *Morse Theory*. 1963.

[21] R. Fry and S. McManus, "Smooth bump functions and the geometry of Banach spaces: a brief survey," *Expositiones Mathematicae*, Vol. 20, No. 2, 2002, pp. 143–183.

[22] W. T. Loring, *An Introduction to Manifolds*. Spring, 2008.

[23] J. Milnor, *Morse Theory*. 1963.

[24] J. E. Marsden and M. West, "Discrete mechanics and variational integrators," *Acta Numerica*, Vol. 10, 2001, pp. 357–514.

[25] N. Nordkvist and A. K. Sanyal, "A Lie Group Variational Integrator for Rigid Body Motion in SE3 with Applications to Underwater Vehicle Dynamics," *49th IEEE Conference on Decision and Control (CDC)*, IEEE, 2010, pp. 5414–5419.